Earth and Planetary Science Letters 546 (2020) 116386

Contents lists available at ScienceDirect

Earth and Planetary Science Letters

www.elsevier.com/locate/epsl

Mantle degassing of primordial helium through submarine ridge flank basaltic basement

Huei-Ting Lin [a,b,*], Marvin D. Lilley [c], John E. Lupton [d], Michael S. Rappé [e]

[a] Institute of Oceanography, National Taiwan University, No. 1, Sec. 4 Roosevelt Road, Taipei City, 10617, Taiwan
[b] Department of Oceanography, School of Ocean and Earth Science and Technology, University of Hawaii, 1000 Pope Road, Honolulu, HI 96822, USA
[c] School of Oceanography, University of Washington, Box 355351, 1503 NE Boat Street, Seattle, WA 98195, USA
[d] Cooperative Institute of Marine Resources Studies (CIMRS), Oregon State University, Newport, OR 97365, USA
[e] Hawaii Institute of Marine Biology, University of Hawaii, P.O. Box 1346, Kaneohe, HI, 96744, USA

ARTICLE INFO

Article history:
Received 28 September 2019
Received in revised form 22 May 2020
Accepted 1 June 2020
Available online 13 July 2020
Editor: L. Derry

Keywords:
^{3}He mantle degassing
ridge flank
abiotic methane
mantle-crust boundary
basement fluids
deep subseafloor

ABSTRACT

The degassing of primordial gases from Earth's interior is evidenced by the high ^{3}He/^{4}He ratios in submarine hydrothermal plumes, vent fluids, and rock samples with mantle origin from active hydrothermal systems in mid-ocean ridges (MOR) and subduction zone volcanism. As the largest aquifer on Earth, the uppermost 40-500 m of permeable submarine ridge flank basement (1-65 million-years-old, Myr) holds ~2% of the ocean volume and accounts for 70% of the seafloor hydrothermal heat flux. However, the degassing of primordial gases through the oceanic ridge flank crust has not yet been directly quantified. Here, we show that high integrity hydrothermal (65 °C) fluids from the sediment-buried 3.5 Myr basaltic crust from the eastern flank of the Juan de Fuca Ridge (JdFR) contain elevated ^{3}He. The ^{3}He/^{4}He for the basaltic fluid is 4.5 ± 0.1 R_a (relative to the air ratio), which is greatly elevated when compared to deep seawater (1.05 R_a), but is half of that observed for high-temperature vent fluids (~8 R_a) emitting from MOR. Only a small fraction of the ^{3}He in ridge flank fluids is derived from the entrainment of high-temperature ridge-axis fluids and is better explained by degassing of the mantle through the mantle-crust boundary. The lower than MOR ^{3}He/^{4}He ratios indicate that radiogenic ^{4}He originates from aged uranium and thorium decay within the mantle as well as from the ridge-flank basalts. The ^{3}He outgassing through warm ridge flanks (4.9 to 36 mol/yr) accounts for 0.7-6% of the global ^{3}He outgassing, exceeded only by degassing through mid-ocean ridges and subduction volcanism. The presence of mantle ^{3}He suggests that the abiogenic methane present in the ridge flank fluids might be mantle-derived. Based on the ^{3}He outgassing flux, a possibly mantle-derived abiotic methane production rate at the ridge flank is estimated to be 0.3–35 × 10^8 mol/yr.

1. Introduction

Helium has two stable isotopes: ^{3}He and ^{4}He. While ^{4}He (α particle) can be replenished by the radioactive decay of uranium and thorium, ^{3}He is almost exclusively primordial. The discovery of a 22% excess of ^{3}He and elevated ^{3}He/^{4}He ratios (1.71×10^{-6}) in deep Pacific Ocean seawater relative to the atmosphere (1.38×10^{-6}) (Clarke et al., 1969) has provided evidence that primordial gases are degassing from Earth's mantle. Extended research has shown that the ^{3}He/^{4}He ratio measured for oceanic volcanic rocks, such as mid-ocean ridge basalts, are eight times higher (1.1×10^{-5}) than that of the atmosphere (Lupton and Craig, 1975; Lupton, 1983; Lupton et al., 1993). Subsequent studies have amply demonstrated the degassing of ^{3}He through hydrothermal venting at mid-ocean ridges and hot spots (Jean-Baptiste et al., 1991, 1998; Kelley et al., 1998; Lupton, 1998; Lupton et al., 1999; Jean-Baptiste et al., 2004; Lupton et al., 2009).

As noted by Mottl (2003), the hydrothermal power output through MOR (1.8 ± 0.4 terawatt, TW) only accounts for 20% of the global power output (9.9 ± 2 TW); ridge flanks ranging in age from 1-65 Myr account for ~70% (7.1 ± 2 TW). The basaltic basement that hosts the aquifer on the eastern flank of the Juan de Fuca Ridge is highly fractured, porous, and permeable, and characterized by similar basement temperatures across over 40 km in distance, which indicates homogenization by vigorous hydrothermal circulation (Davis et al., 1999; Davis and Becker, 2002). Such a large power output implies a high flux of volatiles and other thermally and biogeochemically reactive chemical species that should

* Corresponding author at: Institute of Oceanography, National Taiwan University, No. 1, Sec. 4 Roosevelt Road, Taipei City, 10617, Taiwan.
E-mail address: tinalinht@ntu.edu.tw (H.-T. Lin).

https://doi.org/10.1016/j.epsl.2020.116386
0012-821X/

not be neglected. While the degassing of ^{3}He via ridge flank hydrothermal systems has the potential to be substantial, it has not yet been studied due to difficulties in collecting high quality ridge flank basaltic fluids. Opportunities to collect such samples are now provided by ODP (Ocean Drilling Program) and IODP (Integrated Ocean Drilling Program) CORK (Circulation Obviation Retrofit Kit) observatories installed along the eastern flank of JdFR.

In this study, we report the first direct helium isotope measurements from basaltic basement fluids of the JdFR ridge flank. We discuss the possible sources of the helium isotopes, and calculate the degassing rates by non-magmatic processes. Finally, we use the helium flux to quantify the fluxes of possibly mantle-derived methane (CH_4).

2. Materials and methods

2.1. Sample collection

Submarine ridge flank hydrothermal fluid samples were collected from CORKs installed in ODP borehole 1026B and IODP boreholes U1362A and U1362B (Fisher et al., 2011) (Table 1, Table S1, Fig. S1). At these sites, the basaltic basement is approximately 3.5 Myr, the overlying sediment is 265 m thick, and the basement fluid temperature is ~65 °C (e.g. Davis and Becker, 2002). The overall sampling procedures were described previously (Lin et al., 2014) and detailed in Lin et al. (in revision). Briefly, a matching Aeroquip or Jannasch connector (Wheat et al., 2011) was used to connect the piping of our sampler to the CORK fluid delivery line (FDL) outlet. The fluid intake of the deep horizon in CORK in hole U1362A is located at ~200 meters sub-basement (msb), whereas the shallow horizon opens at 73 msb. Fluid samples were collected through the FDL of the CORK at hole U1362B that opens at 40 msb (Fisher et al., 2005). Our mobile pumping system (MPS) was installed on the front basket of the remotely-operated-vehicle (ROV) Jason, human-occupied-vehicle (HOV) Alvin or on an elevator (Fig. S2) (Lin et al., in revision). The pump pulled basement fluids at a flow rate of 5 L/min (83 ml/sec) through the FDL. Prior to each sample collection, the FDL was flushed with at least 6x its volume with crustal fluid (~50, 70, and 45 min for CORK 1362A shallow, CORK 1362A deep, and CORK 1362B, respectively). During the time of FDL flushing, the basement fluids also filled and flushed the hydrothermal fluid trap reservoir (Lin et al., in revision). The trap was constructed from half-inch-thick polyvinyl chloride (PVC) pipe, and used to retain basement fluid in order to accommodate the fast sampling rate of the gastight sampler (>100 ml/sec; Fig. S2c). The basement fluid trap also allows the collection of hydrothermal fluids (and dissolved gas therein) with Ti-major samplers (Fig. S2d). Prior to deployment, the ~150 ml internal volume of the gastight samplers was evacuated. After a FDL was flushed, the bottle inlet of the gastight sampler was inserted into the fluid trap and opened using a hydraulic actuator by the manipulator of the ROV or HOV. Hydrostatic pressure then rapidly forced the vent fluid sample into the bottle.

At the end of each ROV or HOV dive, the gastight samplers were carefully rinsed with fresh water to remove salts and then stored in the dark at room temperature. Fluids collected with Ti-Major samplers were transferred into pre-evacuated two-arm glass flasks (Fig. S2); fluids in gastight samplers were analyzed directly. Within 8 to 34 days after sample collection, the dissolved gases in the sample fluids were extracted either at the University of Washington or the Helium Isotope Laboratory in Newport, Oregon (Table S2). The extraction protocol was similar to one described previously (Lupton et al., 2006). Briefly, a high vacuum extraction line was equipped with an evacuated glass flask, a low temperature

Table 1
Concentrations and isotopic compositions of helium in basaltic basement fluids from the sedimented Juan de Fuca Ridge flank. The directly measured ($_{meas.}$) and corrected ($_{corr.}$) values are presented.

Site	Intake depth (msb[a])	Dive	Sampling year	Total gas (mmol/kg)	$Ne_{meas.}$ (nmol/kg)	$^4He_{meas.}$ (μmol/kg)	$^3He/^4He_{meas.}$ (Ra)	$Mg_{meas.}$ (mM)	End-member Mg (mM)	Basement fluid end-member in sample (%)	$^4He_{corr.}$ (μmol/kg)	$^3He_{corr.}$ (pmol/kg)	$^3He/^4He_{corr.}$ (Ra)	CH_4[b] (μmol/kg)	$CH_4/^3He$ ($\times10^6$)
1026B	0	A4433	2008	1.11	13	0.052	4.5	2.8	1.9	98	0.050	0.32	4.6	1.9	6.0
1026B	0	A4433	2008	1.10	13	0.052	4.5	2.8	1.9	98	0.050	0.32	4.6	2.0	6.2
1362B	40	J2-569	2011	1.13	12	0.047	4.4	1.8	1.6	100	0.046	0.29	4.5	14	48
1362B	40	J2-710	2013	1.77	21	0.049	4.2	4.5	1.6	94	0.045	0.28	4.5	4.5	15.8
1362A	200	J2-573	2011	1.07	12	0.045	4.3	2.8	2.5	99	0.044	0.27	4.4	5.8	21.7
1362A	200	J2-711	2013	1.27	10	0.045	4.5	5.2	2.5	95	0.044	0.28	4.5	27	99
1362A	200	J2-712	2013	1.20	9	0.043	4.5	7.8	2.5	90	0.043	0.27	4.5	1.8	6.9
1362A	73	J2-714	2013	1.39	14	0.046	4.4	4.3	2.5	96	0.044	0.28	4.5	2.3	8.1
			Average	*1.26*	*13*	*0.047*	*4.4*	*4.0*	*2.1*	*96*	*0.046*	*0.29*	*4.5*	*7.4*	*26.5*
			S.D	*0.23*	*4*	*0.003*	*0.1*	*1.9*	*0.4*	*3*	*0.003*	*0.02*	*0.1*	*9.0*	*32.6*

[a] msb: meter sub-basement.
[b] Lin et al. (2014)

(−60 °C) trap, an all-metal bellows pump, high precision capacitance manometer, a high vacuum pump, and several gastight valves (Fig. S3). The sample was first drawn from the gastight sampler or two-arm glass flask into an evacuated glass flask containing ~1 g of sulfamic acid, which lowered the pH for the extraction of CO_2 and other dissolved gases from the sample fluid into the headspace. The wet gas was subsequently transferred to the low temperature trap to remove water vapor from the total gas. The bellows then pumped the exsolved gases from the drying trap into a calibrated volume. After the pumping was completed, the total amount of dry gas was measured using a high precision capacitance manometer attached to the calibrated volume. Splits of the dry gas were then sealed into glass ampoules. For noble gas measurements, the ampoules were constructed of type 1720 or 1724 aluminosilicate glass that reduced the permeation of helium through the glass (Lupton et al., 2006).

2.2. Analytical methods

Helium and neon concentrations and helium isotope ratios were determined using a special 21-cm radius mass spectrometer with a dual-collector designed for helium isotope determinations at the Helium Isotope Laboratory (Lupton et al., 2006, 2008). The mass spectrometer measurements were standardized by interspersing the sample measurements with measurements of a standard marine air ($^3He/^4He = 1.39 \times 10^{-6}$). For the gastight bottle collections, the detection limit was 0.0018 μmol/kg for helium. For comparison, the average helium concentrations in our samples were 0.047 ± 0.003 μmol/kg (Table 1). The individual helium isotope ratios have an uncertainty of only 0.2% (1-sigma) in $^3He/^4He$ (Lupton et al., 2006).

Helium isotope data are expressed as

$$R = {}^3He/{}^4He \text{ (in atomic ratio)} \quad (1)$$

$$R_a = {}^3He/{}^4He \text{ in the atmosphere} = 1.39 \times 10^{-6} \quad (2)$$

2.3. Data analysis

2.3.1. Basaltic basement fluid end-member correction

Because seawater entrainment can confound the characterization of crustal fluids, a correction is used to determine the end-member (true) concentrations. Since Mg is significantly removed from solution during low temperature (<70 °C) basalt-seawater alteration over long time periods (Seyfried and Bischoff, 1979), sample Mg concentrations are used to quantify the amount of entrained seawater. The lowest Mg concentrations measured from CORKs 1026B, 1362B, and 1362A (1.9 mM, 1.6 mM, and 2.5 mM, respectively) were used as end-member values (Lin et al., 2012, 2014). Due to limited sampling opportunities, no background seawater samples were collected for this study. Instead, we used the ^3He and ^4He concentrations (0.0032 pmol/kg and 0.0022 μmol/kg, respectively) reported for bottom seawater near Gorda Ridge in the Northeast Pacific Ocean (Lupton et al., 1999) as the seawater end-member values for the nearby Juan de Fuca Ridge flank area. Differences between directly-measured and Mg-corrected concentrations were small due to a combination of low entrainment of seawater within our basement fluid samples (i.e. low Mg concentrations) and low concentrations of ^3He and ^4He in bottom seawater. To be consistent with other reported hydrothermal fluid samples, we report the Mg-corrected end-member values and the subsequently corrected ratios.

2.3.2. ^4He production in the basaltic crust

The ^4He production was calculated based on Torgersen and Jenkins (1982) using the production rate (J) equation from Craig and Lupton (Craig and Lupton, 1976). For average tholeiitic concentrations of 0.1 ppm uranium (U) and 0.18 ppm thorium (Th), the ^4He production rate is:

$$J(^4He) = 1.7 \times 10^{-14} \text{ cc/g per year} = 1.7 \times 10^{-8} \text{ μcc/g year} \quad (3)$$

The total amount of ^4He production per gram of tholeiitic basalt can be thus calculated based on the time span. In this calculation, we ignore the small amount of ^3He that may be produced in the crust by second order nuclear reactions from lithium and tritium as described by Morrison and Pine (1955).

Table 2
Estimation of ^3He and ^4He fluxes from warm ridge flank.

Parameters	Ridge axis	Warm ridge flank
Percentage of global hydrothermal power output (%)[a]	20	1.4-8.4
Power output (10^{12} J/s)[a]	1.8 ± 0.4	0.14-0.85
^3He/heat (10^{-18} mol/J)	8.9 ± 3.6	1.1-1.3
^3He flux (mol/yr)	504 ± 206	4.9-36
$^3He/^4He$ (Ra)	8.0 ± 0.5	4.4-4.6
^4He flux (10^6 mol/yr)	45.6 ± 19	0.8-5.6
$CH_4/^3He$ ($\times 10^6$)	0.7-217	6-99
CH_4 flux ($\times 10^8$ mol/yr)	3.5-446	0.3-35
Global ^3He flux (mol/yr)[b]	–	585-672
Contribution to the global ^3He flux (%)	–	***0.7-6***

[a] From Mottl (2003).
[b] From DeVries and Holzer (2019).

2.3.3. Excess heat

The excess heat is calculated by

$$H = C_p \Delta T m \quad (4)$$

where C_p, ΔT, and m are the specific heat (J/kg/K), the temperature anomaly, and the mass of the hydrothermal fluid (e.g. Baker et al., 1987). Here, the specific heat is 4087 J/kg/K for hydrothermal fluid with a temperature of 65 °C, pressure of 300 Mpa, and salinity of 34 g/Kg (Sun et al., 2008; Sharqawy et al., 2010). Please note that the high-temperature (~350 °C) hydrothermal vent fluids that our data are compared with are usually calculated with a specific heat of about 5800 to 6410 J/Kg/K (Elderfield and Schultz, 1996; Lupton et al., 1999). Using equation (4), the excess heat between the 2 °C recharging seawater and the 65 °C warm ridge-flank fluids is 2.4×10^5 J/Kg.

2.3.4. Helium fluxes

Helium degassing flux from the warm ridge flank is calculated based on the average warm ridge flank ^3He/heat relationship of $1.1 \pm 0.1 \times 10^{-18}$ mol/J (Table 2).

$$\Phi_{^3He} = \Phi_{heat} \times {}^3He/heat \quad (5)$$

where Φ_{heat} is the warm ridge flank power output estimated by Mottl (2003) based on global heat flow data. The estimated total power output is 7.1 ± 2 TW through the ridge flanks, from 1 Ma crust to a sealing age of 65 Ma. The power output is consistent with the previous estimate of 6.6 TW by using physical and chemical data (Mottl and Wheat, 1994). Mottl (2003) furthermore used Mg flux and the composition of altered crust to estimate that warm (>40 °C) ridge flank transfers between 2-12% of the ridge flank heat output and is approximately 0.14-0.85 TW.

3. Results

With magnesium (Mg) concentrations ranging from 1.8 to 7.8 mM, basalt-hosted basement fluid samples collected from 2008-2013 along the JdFR flank were depleted in Mg relative to local background seawater (53.7 mM) (Lin et al., 2012). Thus, the

samples used for this research contained between 90% and 100% end-member basaltic basement fluid (Table 1). The percentages of entrained bottom seawater in each sample were used to correct the ^{3}He and ^{4}He concentrations to their end-member basaltic fluid values. Neon concentrations in basement fluid samples ranged from 9-21 nmol/kg, which were elevated compared to that of seawater (7.7 nmol/kg) (Craig and Lupton, 1976). While Ne is depleted in the mantle with He/Ne of 3000 relative to the air He/Ne of 0.29, the 2-13 nmol/kg of excess neon in the hydrothermal samples relative to seawater were thus assumed to be derived from air contamination and correction was applied (Moreira and Kurz, 2013). Despite their collection from different sites and depths, the eight samples used in this study possessed a narrow range of Mg-end-member- and air-corrected ^{3}He and ^{4}He concentrations (0.29 $\pm$ 0.02 pmol/kg and 0.046 $\pm$ 0.003 µmol/kg, respectively; Table 1), resulting in a tight range in ^{3}He/^{4}He of 4.5 $\pm$ 0.1 R_a. To provide a more comprehensive view, we expanded helium isotope, heat, and methane composition of the ridge flank fluids into a data set (Table 3) previously summarized by Sano and Fischer (2013). Additional details of the seawater and air corrections for ^{3}He/^{4}He ratios are given in the Supporting Material.

4. Discussion

4.1. Sources of ^{3}He and ^{4}He in the ridge flank basaltic basement fluids

Ridge flank basement fluids originate from bottom seawater recharging through unsedimented and thinly-sedimented areas of the seafloor. The ^{3}He and ^{4}He in the recharged seawater is likely to remain in solution as the fluids migrate along the hydrothermal flow paths. In contrast to previous predictions of no ^{3}He anomalies in low-temperature (<100 °C) off-ridge vents due to the virtual absence of helium (≪0.00045 µmol/Kg) in hydrothermally altered oceanic crust (Elderfield and Schultz, 1996), our results demonstrate that ridge-flank basement fluids contain at least 20-fold and 90-fold increases in ^{4}He and ^{3}He concentrations, respectively, relative to seawater (Table 3). At 4.5 R_a, the ^{3}He/^{4}He for the basaltic basement fluids is substantially higher than that of recharge seawater of 1.05 R_a (Jean-Baptiste et al., 2004). Thus, during the formation pathways, the flowing fluids must have received additional sources of helium with elevated ^{3}He to ^{4}He ratios.

As described previously, MOR magmatism supplies helium greatly enriched in ^{3}He with a ^{3}He/^{4}He of 8 $\pm$ 1 Ra (e.g. Welhan and Craig, 1983; Jean-Baptiste et al., 1998) (summarized in Table 3). Thus, the entrainment of MOR hydrothermal fluid containing ^{3}He-enriched helium by seawater recharged into the basaltic basement may partially explain the elevated ^{3}He in ridge flank fluids. Based on two-end member mixing, one could obtain a solution with ^{3}He at our measured concentration of 0.29 pmol/kg by mixing 1.9% of 350 °C MOR fluid (^{3}He of 15 pmol/kg; ^{3}He/^{4}He of 8 $\pm$ 1 R_a) (Welhan and Craig, 1983; Jean-Baptiste et al., 1998) and 98.1% of 2 °C seawater (^{3}He of 0.0025 pmol/kg; ^{3}He/^{4}He of 1.05 R_a, Fig. 1) (Craig and Lupton, 1976). However, the ^{3}He/^{4}He of the mixed solution would be 7.58 R_a, which is much higher than the observed value of 4.5 R_a. In addition, the mixed solution would only contain a ^{4}He concentration of 0.027 µmol/kg; an additional 0.019 µmol/kg of ^{4}He is required to meet the measure value of 0.046 µmol/kg in ridge flank crustal fluids.

Two other sources for the helium within the fluid flowing through the ridge flank basement are plausible. Diffusional degassing of primordial ^{3}He from the upper mantle underneath the aged oceanic crust, including the release of helium from basaltic vesicles that trapped primordial ^{3}He during basalt formation could serve as a source (Fig. 2). The ^{3}He concentration measured in gabbro is two orders of magnitude lower than that in the undegassed oceanic crust estimated based on gas-rich popping rocks, confirming that the crust is indeed degassed (Moreira and Kurz, 2013).

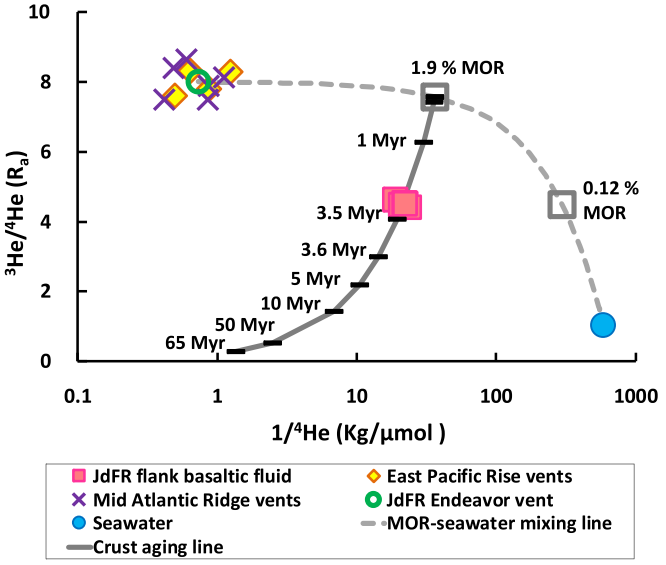

Fig. 1. Helium isotope systematics of ridge flank basaltic fluids, Juan de Fuca Ridge (JdFR) vent fluid from the Endeavour segment (Lilley et al., 1993), East Pacific Rise (Welhan and Craig, 1983) and Mid Atlantic Ridge (Jean-Baptiste et al., 1998, 2004) hydrothermal vent fluids, and seawater. The gray dashed line denotes the mixing between the JdFR mid-ocean ridge hydrothermal fluids or input of primordial ^{3}He from the upper mantle-crust boundary with seawater. For example, to obtain a ^{3}He concentration of 0.29 pmol/Kg, the basaltic fluid may be a mixture of 1.9% of MOR or upper mantle degassing and 98.1% of seawater. Alternatively, to reach a ^{3}He/^{4}He of 4.5 R_a, mixing of 0.12% MOR and 99.88% seawater is needed. The additional input of radiogenic ^{4}He, such as production from uranium and thorium containing minerals, or input of primordial ^{3}He from the upper mantle-crust boundary can also provide the helium isotopes concentrations and isotopic composition in ridge flank basalt. ^{4}He production was calculated based on Torgersen and Jenkins (1982) using the equation of Craig and Lupton (1976). Details in Supporting Information.

Diffusive-loss of helium from basaltic glass and the subsequent stripping of helium out of basalts by circulating seawater has been proposed to be a mechanism to explain the observed low ^{3}He/^{4}He ratios, and low concentrations (Craig and Lupton, 1976). Second, the radioisotope decay of uranium-thorium generates ^{4}He, resulting in elevated ^{4}He in greatly aged crust, and consequently results in low R/R_a (0.1–0.01) (Morrison and Pine, 1955). Based on equation (3), at the rate of production and assuming that radiogenic helium is 100% retained in the rock, the 3.5 Myr-old basalt at our study sites could have accumulated up to 0.0027 µmol/kg-rock of ^{4}He in maximum. Thus, a minimum of 7.3 kg tholeiite is required to produce the 0.019 µmol of ^{4}He needed to meet the observed ^{3}He/^{4}He ratio of 4.5 R_a in 1 kg of hydrothermal solution.

4.2. Flux of helium in warm ridge flanks

The heat fluxes of the basaltic ridge flanks are informative when attempting to evaluate the sources of helium and their fluxes. The decay of ^{238}U, ^{235}U, and ^{232}Th accounts for >75% of the Earth's radiogenic heat (O'nions and Oxburgh, 1983). The radioisotope decay of the uranium and thorium series also generates helium at a characteristic ratio of 10^{12} atoms-^{4}He/W (O'nions and Oxburgh, 1983). Because of the inertness and mobility of helium, the distribution of helium and heat presumably exhibits similar conductive, convective, and diffusive patterns, demonstrated by the relatively constant helium to heat ratios observed in hydrothermal plumes (e.g., Ballentine and Burnard, 2002). Based on this, our previous assumption that the entrainment of 1.9% high-temperature fluid from the ridge axis that accounts for the ^{3}He abundances in the ridge flank fluids is insufficient to provide the heat to raise the fluid temperature to 65 °C at the ridge flank. The addition of heat, ^{3}He, and ^{4}He is required. While the rising temperature of the ridge flank fluids is mostly due to inefficient removal of the latent heat

Table 3
Compilation of helium isotopic compositions in hydrothermal fluids and plume samples from various geological settings around the world.

Hydrothermal site	Type	T (°C)	^{3}He (pmol/kg)	^{3}He/^{4}He (Ra)	^{3}He/heat (10^{-18} mol/J)	$CH_4/^{3}He$ ($\times 10^{6}$)	$^{13}C(CH_4)$ (‰)	References
Juan de Fuca Ridge flank								
Eastern flank of Juan de Fuca	Basaltic basement fluids	~65	0.29 ± 0.02	4.5 ± 0.1	**1.1** ± 0.1	6-99	−26 to −57	This study; Lin et al. (2014)
Juan de Fuca Ridge								
Juan de Fuca (48°N)	Vent	345-400	15-32	8	–	107-217	−55 to −48	Lilley et al. (1993)
Juan de Fuca (45°N)	Event plume	0.035-0.25*	0.005	7.9	3.2-4.3	1-3.2	–	Summarized Lupton et al. (1999); Kelley et al. (1998)
Juan de Fuca (45°N)	Steady-state megaplume	0.04-0.08*	0.006	7.9	14-47	0.7-1.7	–	Summarized Lupton et al. (1999); Kelley et al. (1998)
Axial seamount	Over fresh lava flows	0.02-0.27*	0.0095-0.025	–	22-**75**	–	–	Summarized Lupton et al. (1999)
Cleft Segment (44°40′N)	Vent	280	–	7.7	5.3	–	–	Kennedy (1985)
Cleft Segment (44°48′N)	Steady-state plume	0.01-0.06*	0.0033-0.013	7.9	**1.5**-3.2	–	–	Lupton et al. (1989)
Cleft Segment (44°48′N)	Catastrophic megaplume	0.02-0.27*	0.0027-0.067	7.9	21-43	–	–	Lupton et al. (1989)
East Pacific Rise								
East Pacific Rise (21°N)	Vent	373-355	12.4 ± 2.3	7.8	4.3	3.4-6.5	−18 to −15	Welhan and Craig (1982, 1983)
East Pacific Rise (13°N)	Vent	354-381	21 ± 7	7.6	7.5-15	3.1-3.9	−20 to −17	Merlivat et al. (1987)
East Pacific Rise (11°N)	Vent	347	17.9 ± 8	8.3	9.5	4.5-7.0	–	Welhan et al. (1984)
East Pacific Rise (17-18°S)	Vent	340	9.2 ± 3	8.3	6.2	–	−22 to −24	Charlou et al. (1996); Jean-Baptiste et al. (1997)
Galapagos	Vent	350	–	7.8	5.2	–	–	Jenkins et al. (1978)
MAR								
Menez Gwen (37°50N)	Vent	275-284	20 ± 4	8.7	18	85	−6.8 to −9.1	Charlou et al. (2000)
Lucky Strike (37°11N)	Vent	170-330	10 ± 3.5	8.1	6.5	65	−7.2 to −11	Jean-Baptiste et al. (1998)
Rainbow (36°14N)	Vent	365	25 ± 5	7.5	9.3	100	−16	Jean-Baptiste et al. (2004); Charlou et al. (2002)
Broken Spur (29°N)	Vent	356-364	–	8.9	–	–	−18 to −19	Jean-Baptiste et al. (2004)
TAG (26°N)	Vent	270-366	18.5 ± 2.4	7.5-8.2	7.7-9.3	–	−8 to −8.9	Charlou et al. (1996); Rudnicki and Elderfield (1992)
Back-arc Basin								
North Lau Basin	Translucentsmoker	258-331	1.9-38	7.0-9.8	1.1-22.7	2.9-47	−22 to −24	Konn et al. (2018)
Seawater		2-4	0.0025-0.0032	1.05	–	0.053		Jean-Baptiste et al. (2004); Lupton et al. (1999); Popp et al. (1995)

Table expanded from Sano and Fischer (2013).
* Temperature anomalies.

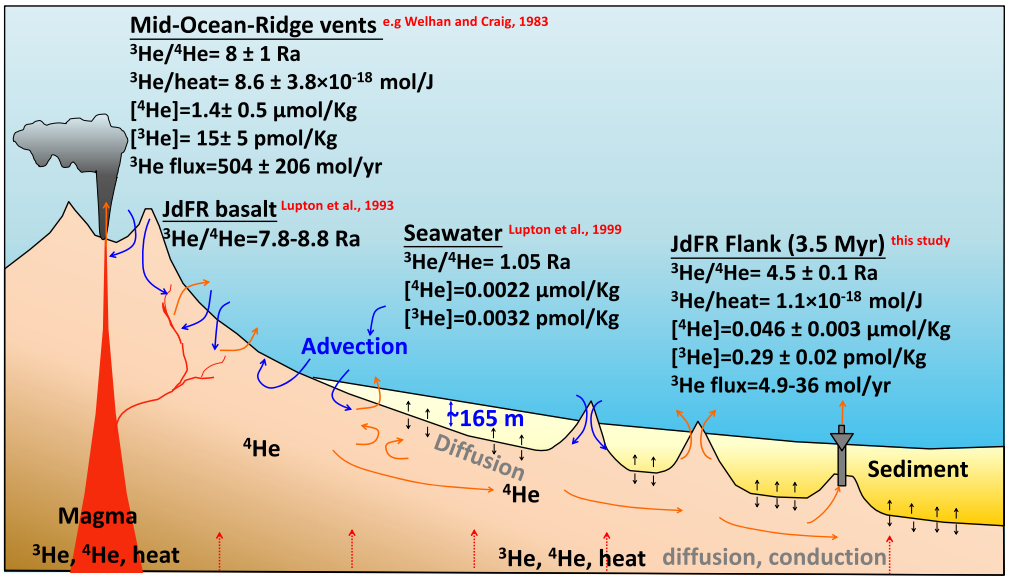

Fig. 2. Schematic drawing showing the formation and flow paths of basaltic basement fluids. In the proposed model, ^3He is degassed from the crust-mantle boundary and through the breaking down of primordial gases trapped in vesicles in the basaltic rocks. ^4He is also produced from the uranium-thorium decay series during the aging of the basaltic crust. Concentrations and isotopic compositions of helium in ridge-flank basaltic fluids (this study), mid-ocean ridge hydrothermal vents (e.g., Welhan and Craig, 1983; Table 3), and seawater (Lupton et al., 1999) are shown for comparison.

generated by cooling of the basalt through the thick impermeable sediment overlying the basaltic basement at our study sites (Davis et al., 1999; Mottl, 2003), the same mechanism likely also traps helium in the basement.

Combining our measured ^3He to ^4He ratios, helium concentrations, and in situ temperature of 65 °C, we obtained ^3He/heat of $1.1 \pm 0.1 \times 10^{-18}$ mol/J and ^4He/heat of $0.2 \pm 0.01 \times 10^{-12}$ mol/J (Table 2). The ridge flank ^3He/heat ratio is the lowest among the reported ratios for submarine hydrothermal systems ($1.1–75 \times 10^{-18}$ mol/J; Table 3), indicating that the ridge flank system has a slow helium extraction or transport rate relative to heat than other systems. The low value observed in the 1986 event plume off the Cleft Segment of the Juan de Fuca Ridge (1.5×10^{-18} mol/J) (Lupton et al., 1989) and other event plumes ($3.2–4.0 \times 10^{-18}$ mol/J) were attributed to rapid emptying of a hydrothermal reservoir or rapid heat extraction from a recently emplaced dike or seafloor lava flow (summarized by Lupton et al., 1999). In contrast, the high values were from plumes over fresh lava flows ($22–75 \times 10^{-18}$ mol/J) and steady-state megaplume ($14-47 \times 10^{-18}$ mol/J) (summarized by Lupton et al., 1999), resulted from episodes of enhanced helium degassing affected by the dynamic conditions within the hydrothermal system related to the age of the system, the water/rock ratios, and the transportation mechanism. For instance, in permeable fault systems, helium can be transported by advection at much faster rates than heat, leading to elevated helium to heat ratios in the hydrothermal solution (Bach et al., 1999). Other samples from mature world-wide MOR hydrothermal systems have ^3He/heat ratios between $4.3-9.5 \times 10^{-18}$ mol/J (e.g., Jenkins et al., 1978) (Table 3 and references therein); the ratios are considered to be the rates for typical ^3He/heat extraction by hydrothermal circulation through mature MOR.

Mechanisms are needed to explain the low ridge flank ^3He/heat and ^4He/heat ratios, which are 1/4 to 1/8 of the ^3He/heat in MOR systems and only 1/12 of the theoretical radioactive decay ^4He/heat of 2.4×10^{-12} mol/J, respectively (O'nions and Oxburgh, 1983). Relative to thermal conductivity, the diffusional transport of helium in the continental crust is estimated to vary by up to three orders of magnitude slower (Torgersen and Clarke, 1992). Because the concentration of uranium in the oceanic crust is relatively constant, the $^3He/^4He$ ratio of the basaltic crust fluid is primarily a function of the ^3He flux from the upper mantle (Ballentine and Burnard, 2002). Thus, we infer that the depressed ^3He/heat and ^4He/heat ratios for the ridge flank fluids result from the lower rate of diffusional transport of helium relative to heat from the upper mantle through the aged oceanic crust.

We estimate that the average global ^3He degassing flux from the warm ridge flank is 4.9 to 36 mol/yr based on the heat output from warm ridge flank (Table 2). Our estimated MOR ^3He flux of 504 ± 206 mol/yr is within the range of recently reported values (585-672 mol/yr; DeVries and Holzer, 2019), validating our ^3He flux approach. In a global context, the ^3He flux of warm-ridge flank is 0.7-6% of the global flux (Table 2 and S3); the uncertainty lies with difficulties in constraining the range of power output for the hydrothermal systems. The significance of the ridge-flank ^3He degassing flux to the global terrestrial degassing is exceeded only by the MOR and subduction volcanism (160-240 mol/yr) (Torgersen, 1989). The diffusive degassing of ^3He from the continental crust-mantle boundary is estimated to be <6.7 mol/yr (Torgersen, 1989), which is at the lower end of our estimated oceanic crust-mantle flux. Provided that the degassing rate of ^3He from the mantle is likely the same, the higher ^3He oceanic crust-mantle flux suggests that oceanic crust is more permeable than its continental counterpart for primordial helium degassing.

4.3. Implications of mantle ^3He on CH_4 biogeochemistry

The degassing flux of primordial ^3He can be used to identify other magmatic volatiles, such as methane (Etiope and Sherwood Lollar, 2013), and to estimate their chemical fluxes from the solid Earth. Understanding the sources and fluxes of high-energy compounds such as CH_4 is critical to understand the subsurface biosphere, as a vast diversity of uncultivated microorganisms in subsurface environments depend on CH_4 to sustain productivity (Colman et al., 2017). While the tight range of the inert helium concentrations and isotopes suggest a homogenized aquifer down to 200 msb, the highly variable hydrogen and methane concentrations and isotopes (Lin et al., 2014; Fig. 3) suggest that microbial activity also plays a role in changing the fluid chemistry. The differences in reactive chemical species such as hydrogen (H_2) and CH_4 (Lin et al., 2014; Fig. 3) among our sampling sites, depths, and

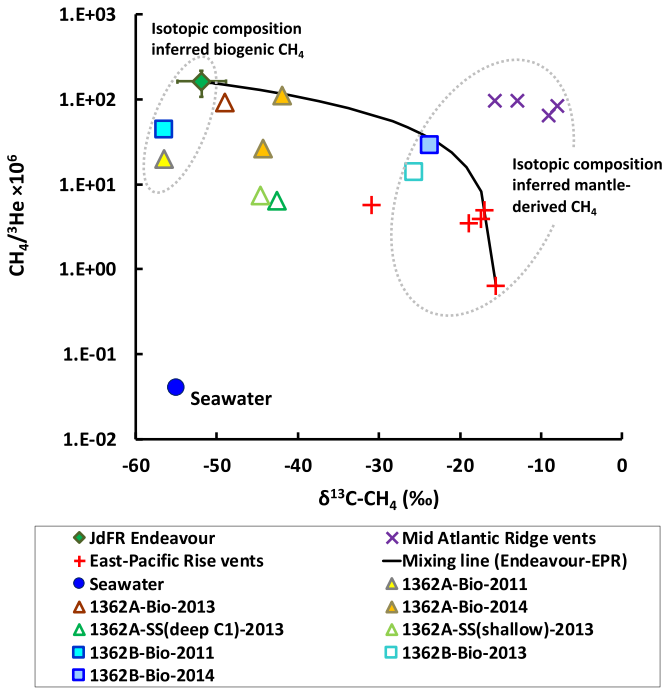

Fig. 3. Helium, methane concentrations and $\delta^{13}C$ of methane in ridge flank basaltic basement fluids (Lin et al., 2014), high-temperature mid-ocean ridge vents, including Mid Atlantic Ridge vents (Jean-Baptiste et al., 1998, 2004) and East-Pacific Rise vents (Welhan and Craig, 1983), sedimented Juan de Fuca Ridge (JdFR) Endeavour hydrothermal vent (Lilley et al., 1993), and seawater (Craig and Lupton, 1976; Popp et al., 1995). Figure modified from Sano and Fischer (Sano and Fischer, 2013). Note: Helium in 2014 JdFR flank fluid samples were not measured but assumed to be the same as 2011 and 2013 samples.

times indicate that the basement fluid mixing rate were slower than the biochemical reaction time.

The $\delta^{13}C$ and the $\delta^{2}H$ of CH_4 preserves information about the carbon and hydrogen feedstock materials and, interestingly, the $\delta^{13}C$ and the $\delta^{2}H$ of CH_4 in some basaltic fluid samples collected from hole U1362B along the JdFR flank are suggestive of an abiogenic origin ($-23‰$ and $-257‰$, respectively) (Lin et al., 2014; and this study). Several mechanisms have been proposed for the abiogenic generation of CH_4 (Etiope and Sherwood Lollar, 2013). For instance, the high-temperature reactions in the mantle, reduction of CO_2 to CH_4 during magma cooling, iron carbonate (siderite) decomposition, Fischer-Tropsch Type reaction of catalytical CO_2 hydrogenation. In a submarine hydrothermal system, the H_2 produced during serpentinization can reduce CO_2 to CH_4 in the hydrothermal fluids (Charlou et al., 2002). Alternatively, CH_4 may form within the vesicles in the gabbro where H_2 reduces magmatic CO_2 as the gabbro cools and the CH_4 is then later extracted from the vesicles during hydrothermal circulation (Kelley and Früh-Green, 1999, 2001; McDermott et al., 2015; Wang et al., 2018; Grozeva et al., 2020). The presence of mantle degassed ^3He in our samples supports the later explanation and that the abiotic CH_4 may entirely or partially be mantle-derived. Indeed, the $CH_4/^3He$ of 6-99 $\times$ 10^6 in the JdFR flank basaltic fluids are bracketed by the $CH_4/^3He$ of the EPR (3.1-7.0 $\times$ 10^6) (e.g. Welhan and Craig, 1983) and the serpentinization influenced MAR (65–100 $\times$ 10^6) (e.g. Charlou et al., 2002), summarized in Table 3.

Adding CH_4 isotopic compositions to the discussion (Fig. 3), all of the JdFR flank fluids are different from the MAR samples and only two of the ridge flank samples fell on or near the mixing line between the biogenic $CH_4/^3He$ from the Juan de Fuca Endeavour vent field and the abiogenic $CH_4/^3He$ from the magmatic end-member—the sediment-free East Pacific Rise (EPR) (Welhan and Craig, 1983). In the biotic-abiotic mixing model, the two samples (1362B, 40 m, 2013 and 2014) contained ~80% of abiotic CH_4 mixed with ~20% biotic CH_4. The rest of the other ridge flank samples have depleted ^{13}C-CH_4 with variable CH_4 concentrations (2.1-29 µmol/kg), and are indicative of more biotic than abiotic CH_4. While the ^3He concentration remains similar in all of the samples, we can infer that the abiotic CH_4 in other samples was utilized by microorganisms or diluted by biogenic CH_4. Nevertheless, based on the ^3He flux calculated previously, an abiotic CH_4 production rate at the ridge flank of 0.3-35 $\times$ 10^8 mol/yr is estimated. The ridge-flank rate is at the low end of the ridge axis (EPR or MAR) magmatic CH_4 flux of 3.5-446 $\times$ 10^8 mol/yr. The ^3He data provide additional insight into the nature of abiotic CH_4 in crustal fluids of the JdFR flank, and allows the first estimation of CH_4 production rates in ridge flank regions of the seafloor.

5. Conclusions

We present the first observation of mantle helium degassing through the ridge flank basaltic aquifer, and estimate the significance of the degassing flux to be surpassed by only degassing through mid-ocean ridges and subduction volcanism. Helium isotope data supports the presence of abiotic CH_4 within the ridge flank basement aquifer of the JdFR, which was previously suggested based on isotopic measures and allows the calculation to estimate the relative abiotic versus biotic CH_4 in the crustal fluids.

Declaration of competing interest

The authors declare that they have no known competing financial interests or personal relationships that could have appeared to influence the work reported in this paper.

Acknowledgements

We dedicate this work to Dr. James P. Cowen, who initiated the integrated multidisciplinary approaches to investigate the biogeochemistry in the basaltic basement subseafloor biosphere. Dr. Cowen contributed significantly in providing research ideas and in developing robust sampling systems used to collect samples for this study, but he sadly passed prior to the final data analysis and manuscript preparation. We thank the chief scientists, captains, crews, and science teams on board R/V *Atlantis* cruises AT15-35, AT18-07, AT26-03, and AT26-18, and the pilots and crews of ROV *Jason II* and HOV *Alvin*. We greatly thank Chih-Chiang Hsieh for his help with the sample collection, Eric Olson for his assistance with the dissolved gas extractions from the gas-tights and CH_4 analysis, and Evans Leigh for his assistance in gas extraction and noble gases analysis. We thank Yuan-Hui (Telu) Li and Te-Fang Lan for insightful comments to improve this manuscript. This work was supported by the National Science Foundation Microbial Observatory Program (MCB06-04014 to J.P. Cowen), Center for Dark Energy Biosphere Investigations (NSF award OCE-0939564 to M.S. Rappé), NSF awards OCE-1260723 and OCE-1851582 (to M.S. Rappé), and the Ministry of Science and Technology of Taiwan award (MOST 105-2119-M-002-034, MOST 107-2611-M-002-002, and MOST 108-2611-M-002-006 to H.-T. Lin). This paper is SOEST contribution number 10999, HIMB contribution 1812 and C-DEBI contribution number 535.

Appendix A. Supplementary material

Supplementary material related to this article can be found online at https://doi.org/10.1016/j.epsl.2020.116386.

References

Bach, W., Naumann, D., Erzinger, J., 1999. A helium, argon, and nitrogen record of the upper continental crust (KTB drill holes, Oberpfalz, Germany): implications for crustal degassing. Chem. Geol. 160, 81–101.

Baker, E.T., Massoth, G.J., Feely, R.A., 1987. Cataclysmic hydrothermal venting on the Juan de Fuca Ridge. Nature 329, 149–151.

Ballentine, C.J., Burnard, P.G., 2002. Production, release and transport of noble gases in the continental crust. Rev. Mineral. Geochem. 47, 481–538.

Charlou, J., Donval, J., Douville, E., Jean-Baptiste, P., Radford-Knoery, J., Fouquet, Y., Dapoigny, A., Stievenard, M., 2000. Compared geochemical signatures and the evolution of Menez Gwen (37°50′N) and Lucky Strike (37°17′N) hydrothermal fluids, south of the Azores Triple Junction on the Mid-Atlantic Ridge. Chem. Geol. 171, 49–75.

Charlou, J.L., Donval, J.P., Fouquet, Y., Jean-Baptiste, P., Holm, N., 2002. Geochemistry of high H_2 and CH_4 vent fluids issuing from ultramafic rocks at the rainbow hydrothermal field (36°14′N, MAR). Chem. Geol. 191, 345–359.

Charlou, J.L., Fouquet, Y., Donval, J.P., Auzende, J.M., Jean-Baptiste, P., Stievenard, M., Michel, S., 1996. Mineral and gas chemistry of hydrothermal fluids on an ultrafast spreading ridge: East Pacific Rise, 17°to 19°S (Naudur cruise, 1993) phase separation processes controlled by volcanic and tectonic activity. J. Geophys. Res., Solid Earth 101, 15899–15919.

Clarke, W.B., Beg, M., Craig, H., 1969. Excess ^{3}He in the sea: evidence for terrestrial primodal helium. Earth Planet. Sci. Lett. 6, 213–220.

Colman, D.R., Poudel, S., Stamps, B.W., Boyd, E.S., Spear, J.R., 2017. The deep, hot biosphere: twenty-five years of retrospection. Proc. Natl. Acad. Sci. 114, 6895–6903.

Craig, H., Lupton, J., 1976. Primordial neon, helium, and hydrogen in oceanic basalts. Earth Planet. Sci. Lett. 31, 369–385.

Davis, E.E., Becker, K., 2002. Observations of natural-state fluid pressures and temperatures in young oceanic crust and inferences regarding hydrothermal circulation. Earth Planet. Sci. Lett. 204, 231–248.

Davis, E.E., Chapman, D.S., Wang, K., Villinger, H., Fisher, A.T., Robinson, S.W., Grigel, J., Pribnow, D., Stein, J., Becker, K., 1999. Regional heat flow variations across the sedimented Juan de Fuca Ridge eastern flank: constraints on lithospheric cooling and lateral hydrothermal heat transport. J. Geophys. Res., Solid Earth 104, 17675–17688.

DeVries, T., Holzer, M., 2019. Radiocarbon and helium isotope constraints on deep ocean ventilation and mantle-^{3}He sources. J. Geophys. Res., Oceans 124, 3036–3057.

Elderfield, H., Schultz, A., 1996. Mid-ocean ridge hydrothermal fluxes and the chemical composition of the ocean. Annu. Rev. Earth Planet. Sci. 24, 191–224.

Etiope, G., Sherwood Lollar, B., 2013. Abiotic methane on Earth. Rev. Geophys. 51, 276–299.

Fisher, A., Wheat, C., Becker, K., Cowen, J., Orcutt, B., Hulme, S., Inderbitzen, K., Turner, A., Pettigrew, T., Davis, E., 2011. Design, deployment, and status of borehole observatory systems used for single-hole and cross-hole experiments, IODP Expedition 327, eastern flank of Juan de Fuca Ridge, pp. 1–15.

Fisher, A.T., Urabe, T., Klaus, A., Scientists, E., 2005. Site U1301. In: Proc. IODP. College Station, TX. Integrated Ocean Drilling Program Management International, Inc., pp. 1–181.

Grozeva, N.G., Klein, F., Seewald, J.S., Sylva, S.P., 2020. Chemical and isotopic analyses of hydrocarbon-bearing fluid inclusions in olivine-rich rocks. Philos. Trans. R. Soc. A 378, 20180431.

Jean-Baptiste, P., Bougault, H., Vangriesheim, A., Charlou, J., Radford-Knoery, J., Fouquet, Y., Needham, D., German, C., 1998. Mantle ^{3}He in hydrothermal vents and plume of the Lucky Strike site (MAR 37°17′N) and associated geothermal heat flux. Earth Planet. Sci. Lett. 157, 69–77.

Jean-Baptiste, P., Charlou, J., Stievenard, M., Donval, J., Bougault, H., Mevel, C., 1991. Helium and methane measurements in hydrothermal fluids from the Mid-Atlantic Ridge: the Snake Pit site at 23°N. Earth Planet. Sci. Lett. 106, 17–28.

Jean-Baptiste, P., Dapoigny, A., Stievenard, M., Charlou, J., Fouquet, Y., Donval, J., Auzende, J., 1997. Helium and oxygen isotope analyses of hydrothermal fluids from the East Pacific Rise between 17°S and 19°S. Geo Mar. Lett. 17, 213–219.

Jean-Baptiste, P., Fourré, E., Charlou, J.-L., German, C.R., Radford-Knoery, J., 2004. Helium isotopes at the Rainbow hydrothermal site (Mid-Atlantic Ridge, 36°14′N). Earth Planet. Sci. Lett. 221, 325–335.

Jenkins, W., Edmond, J., Corliss, J., 1978. Excess ^{3}He and ^{4}He in Galapagos submarine hydrothermal waters. Nature 272, 156–158.

Kelley, D.S., Früh-Green, G.L., 1999. Abiogenic methane in deep-seated mid-ocean ridge environments: insights from stable isotope analyses. J. Geophys. Res., Solid Earth 104, 10439–10460.

Kelley, D.S., Früh-Green, G.L., 2001. Volatile lines of descent in submarine plutonic environments: insights from stable isotope and fluid inclusion analyses. Geochim. Cosmochim. Acta 65, 3325–3346.

Kelley, D.S., Lilley, M.D., Lupton, J.E., Olson, E.J., 1998. Enriched H_2, CH_4, and ^{3}He concentrations in hydrothermal plumes associated with the 1996 Gorda Ridge eruptive event. Deep-Sea Res., Part 2 45, 2665–2682.

Kennedy, B., 1985. Noble gases in vent fluids from the Juan de Fuca Ridge. Eos Trans. AGU 66, 929.

Konn, C., Donval, J., Guyader, V., Roussel, E., Fourré, E., Jean-Baptiste, P., Pelleter, E., Charlou, J., Fouquet, Y., 2018. Organic, gas, and element geochemistry of hydrothermal fluids of the newly discovered extensive hydrothermal area in the Wallis and Futuna region (SW Pacific). Geofluids 2018.

Lilley, M., Butterfield, D., Olson, E., Lupton, J., Macko, S., McDuff, R., 1993. Anomalous CH_4 and NH_4^+ concentrations at an unsedimented mid-ocean-ridge hydrothermal system. Nature 364, 45–47.

Lin, H.-T., Cowen, J.P., Olson, E.J., Amend, J.P., Lilley, M.D., 2012. Inorganic chemistry, gas compositions and dissolved organic carbon in fluids from sedimented young basaltic crust on the Juan de Fuca Ridge flanks. Geochim. Cosmochim. Acta 85, 213–227.

Lin, H.-T., Cowen, J.P., Olson, E.J., Lilley, M.D., Jungbluth, S.P., Rappé, M.S., Wilson, S.T., 2014. Dissolved hydrogen and methane in the oceanic basaltic biosphere. Earth Planet. Sci. Lett. 405, 62–73.

Lin, H.-T., Hsieh, C.-C., Repeta, D.J., Rappé M.S., in review. Sampling of basement fluids via Circulation Obviation Retrofit Kit (CORK) for dissolved gases, seafloor fixation experiment, and organic characterization. MethodsX.

Lupton, J.E., 1983. Terrestrial inert gases-isotope tracer studies and clues to primordial components in the mantle. Annu. Rev. Earth Planet. Sci. 11, 371–414.

Lupton, J., 1998. Hydrothermal helium plumes in the Pacific Ocean. J. Geophys. Res., Oceans 103, 15853–15868.

Lupton, J., Craig, H., 1975. Excess ^{3}He in oceanic basalts: evidence for terrestrial primordial helium. Earth Planet. Sci. Lett. 26, 133–139.

Lupton, J., Baker, E., Massoth, G., 1989. Variable ^{3}He/heat ratios in submarine hydrothermal systems: evidence from two plumes over the Juan de Fuca ridge. Nature 337, 161–164.

Lupton, J.E., Graham, D.W., Delaney, J.R., Johnson, H.P., 1993. Helium isotope variations in Juan de Fuca Ridge basalts. Geophys. Res. Lett. 20, 1851–1854.

Lupton, J.E., Baker, E.T., Massoth, G.J., 1999. Helium, heat, and the generation of hydrothermal event plumes at mid-ocean ridges. Earth Planet. Sci. Lett. 171, 343–350.

Lupton, J., Butterfield, D., Lilley, M., Evans, L., Nakamura, K.i., Chadwick Jr, W., Resing, J., Embley, R., Olson, E., Proskurowski, G., 2006. Submarine venting of liquid carbon dioxide on a Mariana Arc volcano. Geochem. Geophys. Geosyst. 7.

Lupton, J., Lilley, M., Butterfield, D., Evans, L., Embley, R., Massoth, G., Christenson, B., Nakamura, K.i., Schmidt, M., 2008. Venting of a separate CO_2-rich gas phase from submarine arc volcanoes: examples from the Mariana and Tonga-Kermadec arcs. J. Geophys. Res., Solid Earth 113.

Lupton, J.E., Arculus, R.J., Greene, R.R., Evans, L.J., Goddard, C.I., 2009. Helium isotope variations in seafloor basalts from the northwest Lau Backarc Basin: mapping the influence of the Samoan hotspot. Geophys. Res. Lett. 36.

McDermott, J.M., Seewald, J.S., German, C.R., Sylva, S.P., 2015. Pathways for abiotic organic synthesis at submarine hydrothermal fields. Proc. Natl. Acad. Sci. 112, 7668–7672.

Merlivat, L., Pineau, F., Javoy, M., 1987. Hydrothermal vent waters at 13°N on the East Pacific Rise: isotopic composition and gas concentration. Earth Planet. Sci. Lett. 84, 100–108.

Moreira, M., Kurz, M., 2013. Noble Gases as Tracers of Mantle Processes and Magmatic Degassing, the Noble Gases as Geochemical Tracers. Springer, pp. 371–391.

Morrison, P., Pine, J., 1955. Radiogenic origin of the helium isotopes in rock. Ann. N.Y. Acad. Sci. 62, 71–92.

Mottl, M.J., 2003. Partitioning of energy and mass fluxes between mid-ocean ridge axes and flanks at high and low temperature. In: Halbach, P.E., Tunnicliffe, V., Hein, J.R. (Eds.), Energy and Mass Transfer in Marine Hydrothermal Systems. Dahlem University Press, Berlin, pp. 271–286.

Mottl, M.J., Wheat, C.G., 1994. Hydrothermal circulation through midocean ridge flanks-fluxes of heat and magnesium. Geochim. Cosmochim. Acta 58, 2225–2237.

O'nions, R., Oxburgh, E., 1983. Heat and helium in the Earth. Nature 306, 429.

Popp, B.N., Sansone, F.J., Rust, T.M., Merritt, D.A., 1995. Determination of concentration and carbon isotopic composition of dissolved methane in sediments and nearshore waters. Anal. Chem. 67, 405–411.

Rudnicki, M., Elderfield, H., 1992. Helium, Radon and manganese at the TAG and Snakepit hydrothermal vent fields, 26°and 23°N, mid-Atlantic ridge. Earth Planet. Sci. Lett. 113, 307–321.

Sano, Y., Fischer, T.P., 2013. The analysis and interpretation of noble gases in modern hydrothermal systems. In: The Noble Gases as Geochemical Tracers. Springer, pp. 249–317.

Seyfried, W.E., Bischoff, J., 1979. Low temperature basalt alteration by sea water: an experimental study at 70°C and 150°C. Geochim. Cosmochim. Acta 43, 1937–1947.

Sharqawy, M.H., Lienhard, J.H., Zubair, S.M., 2010. Thermophysical properties of seawater: a review of existing correlations and data. Desalin. Water Treat. 16, 354–380.

Sun, H., Feistel, R., Koch, M., Markoe, A., 2008. New equations for density, entropy, heat capacity, and potential temperature of a saline thermal fluid. Deep-Sea Res., Part 1 55, 1304–1310.

Torgersen, T., 1989. Terrestrial helium degassing fluxes and the atmospheric helium budget: implications with respect to the degassing processes of continental crust. Chem. Geol., Isot. Geosci. Sect. 79, 1–14.

Torgersen, T., Clarke, W., 1992. Geochemical constraints on formation fluid ages, hydrothermal heat flux, and crustal mass transport mechanisms at Cajon Pass. J. Geophys. Res., Solid Earth 97, 5031–5038.

Torgersen, T., Jenkins, W., 1982. Helium isotopes in geothermal systems: Iceland, the geysers, raft river and steamboat springs. Geochim. Cosmochim. Acta 46, 739–748.

Wang, D.T., Reeves, E.P., McDermott, J.M., Seewald, J.S., Ono, S., 2018. Clumped isotopologue constraints on the origin of methane at seafloor hot springs. Geochim. Cosmochim. Acta 223, 141–158.

Welhan, J., Craig, H., 1982. Abiogenic methane in mid-ocean ridge hydrothermal fluids. In: Gwillian, W.J. (Ed.), Deep Source Gas Workshop Tech. Proc., pp. 122–128.

Welhan, J., Craig, H., 1983. Methane, hydrogen and helium in hydrothermal fluids at 21°N on the East Pacific Rise. In: Rona, P.A., Boström, K., Laubier, L., Smith, K.L. (Eds.), Hydrothermal Processes at Seafloor Spreading Centers, pp. 391–411.

Welhan, J., Craig, H., Kim, K., 1984. Hydrothermal gases at 11°N and 13°N on the East Pacific Rise. Eos 65, 45.

Wheat, C.G., Jannasch, H.W., Kastner, M., Hulme, S., Cowen, J.P., Edwards, K.J., Orcutt, B.N., Glazer, B.T., 2011. Fluid sampling from oceanic borehole observatories: design and methods for CORK activities (1990-2010). In: Proc. IODP, vol. 327, pp. 1–36.